Temperature influence on the formation of Langmuir monolayers with Ni arachidic acid and Ni arachidate clusters

Iliya A. Gorbachev, Andrey V. Smirnov, Iren E. Kuznetsova, Vladimir V. Kolesov
Kotelnikov Institute of Radioengineering and Electronics of Russian Academy of Science, http://www.cplire.ru/
Moscow 125009, Russian Federation
E-mail: iliyagor36@gmail.com, andre-smirnov-v@yandex.ru, kuziren@yandex.ru, kvv@cplire.ru

Abstract: **Changing the temperature of the aqueous subphase makes it possible to control the absorption rate of metal ions dissolved in the aqueous subphase by the Langmuir monolayer. This affects the morphology of the Langmuir monolayers formed at an elevated temperature of the aqueous subphase. An adsorption of metal ions by a monolayer leads to the formation of nanoclusters under it. In the present work the process of formation of nickel arachidate (NiArch) clusters under a Langmuir monolayer of arachidic acid (AA) at different temperatures was studied. The process of adsorption of Ni^{2+} ions and formation of clusters of nickel salts under a Langmuir monolayer of arachidic acid (AA) at different temperatures was studied. The subphase temperature was changed in the range of 10 to 30°C with a step of 4°C. The formed films were transferred on the solid substrates. The morphology of the corresponding LB films transferred onto a solid substrate was analyzed by atomic force microscopy. It was found that an increase in the subphase temperature leads to changing in the process of Ni^{2+} ions adsorption by Langmuir monolayer of AA. It was shown that subphase temperature influenced the compressibility of a monolayer, the area occupied by one molecule in the Langmuir monolayer of NiArch, and the morphology of Langmuir-Blodgett (LB) films formed on their basis. An increasing of subphase temperature leads to increase in the number of NiArch clusters in the LB AA film and a decrease in their size. This is due to a change in the rate of growth and dissolution of NiArch clusters with a temperature change. The distribution of NiArch clusters in the resulting film was random. The results obtained are of great importance for the possibility of the creation of multilayer composite coatings with controlled characteristics.**

Keywords: **Langmuir monolayers, Ni arachidate clusters, arachidic acid, monolayer morphology, atomic force microscopy, Langmuir-Blodgett films**

UDC 539.23, 544.032.7

CONTENTS

1. INTRODUCTION

The Langmuir-Blodgett (LB) technology is a promising method for the formation of thin highly organized films based on amphiphilic molecules or nanoparticles stabilized by them [1-3]. The use of surfactants with selectivity to various agents makes it possible to create thin films with sensory properties [4-6]. As is known, the developed surface of LB films allows them to be used, among other things, as sensitive adhesive coatings [7]. In this case, the problem of increasing the specific surface area of such a film is of particular relevance. One of the approaches to the creation of LB films with a developed morphology is the formation of mixed Langmuir monolayers with embedded nanoscale objects [8,9]. Two approaches are used to form such films. The first approach is used in the formation of mixed layers with nanoparticles synthesized in a separate technological cycle [10,11]. The second one is to obtain nanoparticles during the formation of the film itself [12]. A monolayer of surfactant molecules is modified by metal ions dissolved in the aqueous subphase to reach this purpose. The adsorption of metal ions by a Langmuir monolayer leads to the appearance and growth of clusters under its surface. In this case, an exchange reaction occurs between the polar part of the surfactant molecule and ions dissolved in the aqueous subphase [13,14]. As is known, the physicochemical properties of the formed monolayers depend on the acidity and temperature of the subphase, as well as on the concentration of metal ions in the subphase [15]. This is clearly seen in the analysis of the compression isotherms of the created monolayers. The effect of Cu^{2+}, Ca^{2+}, and Ni^{2+} ions on phase transitions and the morphology of fatty acid monolayers was studied in [16-20]. The effect of the adsorption of Ba^{2+} ions on the morphology and phase transitions in mixed monolayers of behenic and stearic acids was studied in [21]. It was shown that the adsorption of metal ions can lead to the disappearance of the liquid phase of the monolayer [16,17], an increase in its length [18], and a change in the shape of the compression isotherm after the collapse of the monolayer [21,22]. The effect of temperature and acidity on the stability of monolayers of oleic acid and bovine serum albumin in the presence of Ca^{2+} ions was studied in [23]. It should be noted that the adsorption of metal ions from the subphase should affect the morphology of the Langmuir-Blodgett film transferred onto a solid substrate. In particular, the authors of [19, 24] studied the effect of the adsorption of Ni^{2+} and Cd^{2+} ions on the morphology of the Langmuir–Blodgett film of arachidic acid. It was shown that in this case the area occupied by arachidic acid molecules in the film changes. The possibility of forming a multilayer film structure during the collapse of a monolayer on the subphase surface was also demonstrated [21,22].

The morphology and surface-active properties of monolayers can also be affected by external electric and magnetic fields. For example, an external magnetic field applied to a monolayer of arachidic acid during the adsorption of iron ions makes it possible to control the growth direction of iron nanoparticles under the monolayer [25]. Thus, by changing the adsorption parameters of metal ions, it is possible to influence the morphology of Langmuir-Blodgett films.

The formation of metal nanoparticles under the surface of a monolayer leads to the creation of inhomogeneity in the morphology of films obtained on its basis. Similar inhomogeneities are formed during the synthesis of nanoparticles in a mixed monolayer [14]. It should be noted that based on the above-mixed monolayers doped with metal ions, it is possible to create composite coatings with different properties.

An analysis of the literature showed that temperature is the least studied factor influencing the properties of Langmuir monolayers and the growth dynamics of nanoparticles under them. This is because temperature affects both the

monolayer formation process and the dynamics of the nanoparticle formation reaction. It is a challenge to study these processes separately from each other. It should also be noted that controlling the number of nanoclusters of metals and their compounds in Langmuir monolayers is an important problem for their practical application as conductive or sensor coatings. However, the effect of temperature on this parameter has not yet been practically studied.

The ordered films with incorporated magnetic nanoparticles made of such materials as nickel, iron, and cobalt have the particular interest. It should be noted that nickel nanoparticles have a noticeable antibacterial effect against resistant bacterial cultures [26]. Using the effect of temperature on the properties of LB films based on fatty acids containing similar nanoparticles, it is possible to form films with a more developed surface. Such films can be further used as sensor coatings in various sensors and can be effectively used in food safety technologies.

Thus, the purpose of this work was to study the mechanism of the formation of nickel arachidate (NiArch) clusters under a Langmuir monolayer of arachidic acid (AA) at different temperatures and to investigate the morphology of LB films based on the resulting mixed monolayers.

2. EXPERIMENTAL PART
2.1. FORMATION OF LANGMUIR MONOLAYERS
AA [$CH_3(CH_2)_{18}COOH$, 99%], chloroform (PAI, filtered), chloride nickel powder [$NiCl_2 \times 6H_2O$, 99.9%], sodium citrate [$Na_3C_6H_5O_7 \times 2H_2O$], and citric acid [$C_6H_8O_7 \times H_2O$] were purchased from Sigma Aldrich. Deionized water (electrical resistivity of 18 M$\Omega \cdot$cm) was obtained by means of ultrapure water purification system Milli-Q plus (Millipore Corp.).

All LB monolayers were produced with an automated LB KSV NIMA 622 (KSV Instruments Ltd., Finland) with a work square of 1200 cm^2. An aqueous solution of $NiCl_2$ (4 mM) was used as a subphase. The pH value of the subphase was fixed at pH = 5.8 to prevent the creation of $Ni(OH)_2$ and nickel-based tetranuclear hydrocomplex. The formation process of these compounds was a pH-dependence process that took a flow at pH value of more than 7 [27]. An acetate buffer (0.1 M; 22.67 g

sodium citrate and 4.402 g citric acid ratio per liter of water) was used to adjust the acidity.

In the Langmuir-Blodgett technology, a continuous monomolecular layer is preliminarily formed on the subphase surface. Then, using a movable barrier, the monolayer is compressed to obtain a continuous film with close packing of molecules. Here the molecule mean area A is approximately equal to the cross-sectional area of the molecule, and hydrophobic hydrocarbon chains are oriented almost vertically. At the final stage, the formed monolayer was transferred onto the surface of the substrate at a constant surface pressure of 35 mN/m by using the Langmuir-Schaeffer method. The transferring ratio was equal to 0.9.

The influence of time on the process of nickel ion binding with an arachidic acid monolayer was studied in [19]. It has been shown that the incorporation of Ni^{2+} ions into the AA monolayer occurs even in the gas phase before the barriers begin to move. In the present work, the formation time of NiArch clusters was constant for each of the chosen temperatures and amounted to 75 minutes. In particular, the solvent evaporated from the water surface for 15 minutes, and then, for 60 minutes, the monolayer was compressed until a transfer pressure of 35 mN/m was reached.

A solution of arachidic acid (1 mM) in chloroform was used to form a monolayer. An aliquot of the solution (50 μL) was dropped onto the surface of the subphase, kept for 15 min, and compressed by movable barriers at a constant compression rate. The barrier compression rate was 20 cm^2/min. The influence of temperature on the properties of the Langmuir monolayer was studied in the range from 10 to 30°C with a step of 4°C. The subphase temperature was controlled by a Brinkmann Lauda RC6 RCS thermostat with an accuracy of ± 0.1°C.

2.2. ANALYSIS OF THE COMPRESSION ISOTHERMS
In the Langmuir-Blodgett technology, the state of the monolayer is described by the compression isotherm π-A, which reflects the ratio between the surface pressure of the barrier π and the molecule mean area A at a constant temperature T. It should be noted that the phase state of the amphiphilic substance monolayer localized at the "subphase-gas" interface is determined by the adhesive-cohesive balance of forces in the "subphase-monolayer"

system and depends on the nature of the substance and the structure of its molecules, temperature T, and subphase composition [28]. The linear sections on the π-A compression isotherm, corresponding to the compression of the monolayer in different phase states, are characterized by the area per molecule in the monolayer obtained by extrapolating the linear section to the abscissa axis ($\pi = 0$ mN/m). Thus, gaseous, liquid-expanded, tilted-condensed, and untilted-condensed phases of the monolayers are distinguished on the compression isotherm. These monolayers are in different states of aggregation.

The next parameters were used to assess the effect of temperature on the compression isotherms [15,29]:

A_{C0} and A_{L0} are the molecule mean area of AA molecule in the untilted-condensed, and tilted-condensed phases of a pure monolayer, respectively, and $A_{C0} = 20.1$ Å, $A_{L0} = 23.5$ Å at $T = 22°C$;

A_{CN} and A_{LN} are the molecule mean area of AA molecule in a monolayer formed on a subphase with dissolved Ni^{2+} ions in the untilted-condensed, and tilted-condensed phases, respectively, and $\Delta A_d = A_{CN} - A_{C0}$;

ΔA_0 is the length of the area of the tilted-condensed phase of the AA monolayer on the compression isotherm. It is determined as $\Delta A_0 = A_{L0} - A_{C0}$, $\Delta A_N = A_{LN} - A_{CN}$;

k_C and k_L are the compression modulus of the monolayer in the untilted-condensed, and tilted-condensed phases, respectively.

The approach proposed by Vollhardt and Feinerma was used for quantitative assessment of k_C and k_L [28]. This approach is based on the assumption that the change in the slope of the linear sections of the compression isotherm corresponds to phase transitions in the monolayer. In this case, the change in compression modulus (k) of the monolayer can be estimated from:

$$k = -A_0 \frac{d\pi}{dA}. \qquad (1)$$

Here A_0, A, π, are the area occupied by the molecule in the corresponding phase, the molecule mean area, the surface pressure, respectively.

The phase transition points appearing at the formation of a monolayer and the values of the corresponding molecule mean areas per molecule are usually determined using the dependence of the change in k versus A [30].

2.3. MORPHOLOGY STUDIES OF THE MONOLAYERS TRANSFERRED ONTO THE SOLID SURFACE

Monolayers formed at a surface pressure of 35 mN/m were transferred using the Langmuir-Schaeffer method onto the surface of a hard glass coverslip with a size of 24 mm×24 mm and a roughness of ~0.6 nm (Carl ROTH Gmbh & Co, Germany). In this case, the monolayer is in the untilted-condensed phase at any temperature. Atomic force microscopy (AFM) Integra Spectra probe station (NT-MDT, Russia) was used to study the morphology of AA monolayers modified with NiArch clusters. Before AFM measurements, the samples were stored in a desiccator for 24 h at room temperature to evaporate water. AFM scans of 40 μm×40 μm and 5 μm×5 μm were used for the estimation of the NiArch cluster average area and its thickness, respectively. AFM images were analyzed using the ImageJ v.1.53e and Gwyddion v.2.61 programs. It allowed to perform statistical processing and determining the average geometric parameters of the cluster.

3. RESULTS AND DISCUSSION
3.1. INFLUENCE OF Ni^{2+} IONS
Compression isotherms of AA monolayers formed on the surface of the aqueous subphase at $T = 22°C$ in the presence and the absence of dissolved Ni^{2+} ions are shown in **Fig. 1.** Adsorption of

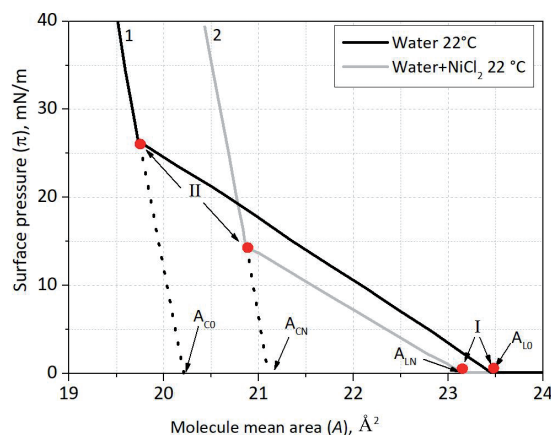**Fig. 1.** *Typical compression isotherms of AA monolayer on the surface of aqueous subphase consisted of (1) pure water and (2) aqueous solution of NiCl$_2$ (4mM) obtained at T = 22°C. Points (I) and (II) indicate the phase transitions from coexisting of the gaseous and liquid-expanded phases to tilted-condensed phase (I) and from tilted-condensed to untilted-condensed phase (II) of the film, respectively.*

Ni^{2+} ions from the subphase with a $NiCl_2$ powder concentration not exceeding 1 mM affects the behavior of compression isotherms but does not lead to significant changes in the morphology of AA monolayers at any temperature of the subphase [30,31]. In this regard, the concentration of Ni^{2+} ions in the subphase was fixed at the level of 4 mM. It is necessary to note that the incorporation of nickel ions into the monolayer is as follows. The water-soluble salt $NiCl_2$ dissociates into Ni^{2+} and $2Cl^-$ ions. This process leads to the formation of water-insoluble hydroxide $Ni(OH)_2$ at an acidity above 7 [32]. At lower acidities, the complex compound $Ni(OH)_2$ is formed, which was observed in the present work. Negatively charged AA-ions are formed as a result of the polarization of the hydrophilic parts of AA molecules at their interaction with water molecules. This leads to the formation of a nickel arachinate salt (NiArch) and an increase in the area occupied by one AA molecule in the untilted-condensed phase (A_0) [32]. For this reason, Ni can be attributed to the group of metals, the use of which has an expanding effect when it is adsorbed by a Langmuir monolayer.

Points (I) and (II) correspond to the phase transitions in the AA monolayer coexisting of the gaseous and liquid-expanded phases – "tilted-condensed phase" (I) and "untilted-condensed phase" (II). The adsorption of Ni^{2+} ions in the LB film from the subphase leads to an increase in the area occupied by the AA molecule by 3.6% (from 20.1 Å² to 20.9 Å²) and decrease in the length of the tilted-condensed phase region by 32%. The decrease in the length of the liquid phase region on the compression isotherm during the adsorption of Ni^{2+} ions agrees with the results of [18,30].

The presence of Ni^{2+} ions affects the average area occupied by an AA molecule in the untilted-condensed phase of a monolayer (A_{C0}). This change is more noticeable than the change in the molecule mean area in the tilted-condensed phase of the monolayer (A_{L0}). The change in the areas occupied by the AA molecule in the pure monolayer and the monolayer modified with NiArch clusters is 0.8 Å² and 0.2 Å² for the untilted-condensed and tilted-condensed phases of the AA monolayer, respectively.

3.2. INFLUENCE OF TEMPERATURE ON THE ISOTHERMS

Compression isotherms of AA monolayers formed on the subphase without dissolved Ni^{2+} ions at different subphase temperatures are shown in **Fig. 2**. It can be seen that a change in the subphase temperature from 10°C to 26°C leads to a change in the monolayer collapse pressure from 60 to 52 mN/m, and the molecule mean area (A_0) does not change. An increase in temperature to 30°C leads to a decrease in A_0 to 20.0 Å² and an increase in the length of the tilted-condensed phase of the AA monolayer from 1.9 Å² to 4.4 Å². A similar effect of decreasing the monolayer collapse pressure and the A_0 value was described earlier for monolayers of CdSe quantum dots stabilized with oleic acid. This effect was explained by a decrease in monolayer stability due to an increase in the thickness of the quiescent layer [33].

Compression isotherms of AA monolayers formed on the subphase in the presence of Ni2+ ions (a) and the dependences of changes in their compressibility modulus on the area occupied by one AA molecule (b) at various temperatures are shown in **Fig. 3**. Two linear segments corresponding to the transition of the AA monolayer from the coexisting of the gaseous and liquid-expanded phases to the tilted-condensed phase (I-II) and from the tilted-condensed to the untilted-condensed phase (III-IV) are shown in Fig. 3*b*. The line segment II-III in Figures 3*a* and 3*b* has corresponded to the
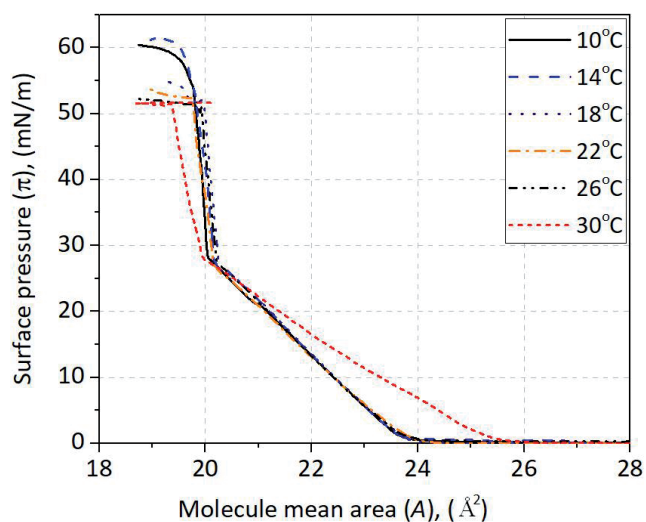

Fig. 2. *Compression isotherms of arachidic acid monolayers formed at the different subphase temperature in the absence of dissolved Ni^{2+} ions.*
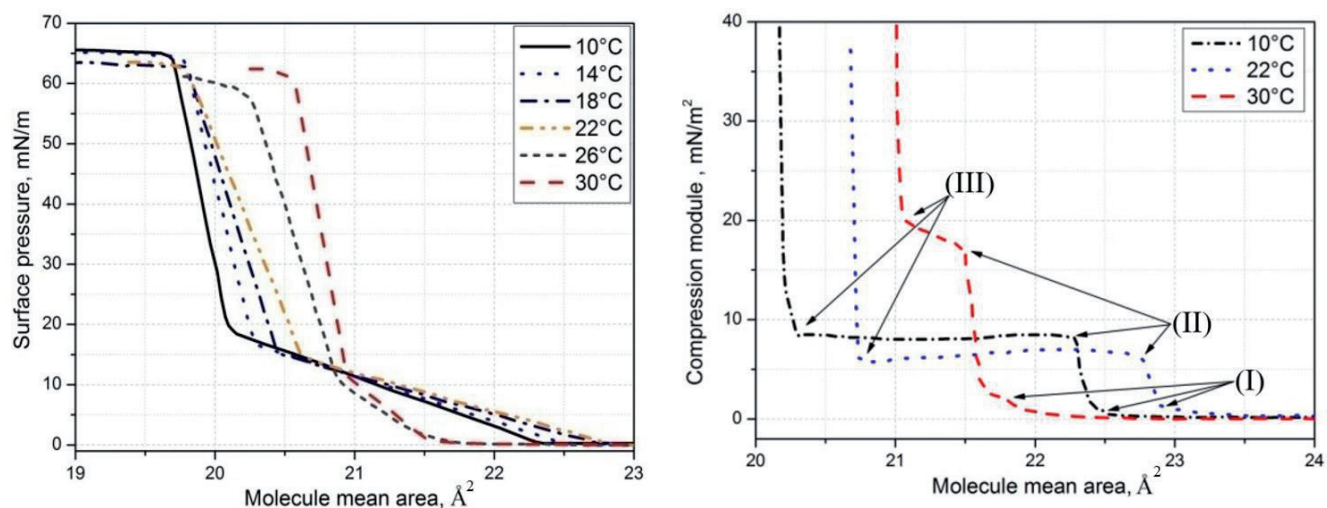
Fig. 3. (a) Influence of the subphase temperature on the compression isotherms of AA monolayer in the presence of Ni^{2+} ions in the subphase (4mM). (b) The compression isotherms were obtained using the subphase with 10°C, 22°C, and 30°C temperatures. The segments I-II and III-IV in Fig. 3b are corresponded to the transition of the AA monolayer from the phase of coexisting of the gaseous and liquid-expanded phases to the tilted-condensed phase and from the tilted-condensed to the untilted-condensed phase, respectively. The linear segment II-III in Figures 3a and 3b is corresponded to the tilted-condensed phase of the AA monolayer.

tilted-condensed phase of the AA monolayer. The temperature influence on the AA monolayers with embedded NiArch nanoparticles is presented in **Table 1.** It is possible to see that an increase in the subphase temperature reduces the length of the tilted-condensed phase region and the difference between the molecule mean areas of AA molecules in the monolayer. In this case, the compression modulus of the tilted-condensed and untilted-condensed phases of the AA monolayer increases.

From Fig. 3b it is possible to see that an increase in the temperature of the subphase leads to an increase in the slope of the section of the II-III

Table 1

The temperature influence on the AA monolayers with embedded NiArch nanoparticles: the difference between mean area of AA in the pure monolayer and in the monolayer modified by NiArch (ΔA_d), length of liquid phase (ΔA_0), monolayer compressibility modulus in untilted-condensed (k_C) and tilted-condensed (k_L) phases.

Tempe-rature, °C	Condensed phase		Liquid phase		ΔA_0, Å²	ΔA_d, Å²
	A_{CN}, Å²	$k_C \times 10^3 mN/m$	A_{LN}, Å²	$k_L \times 10^3 mN/m$		
10	20.2	0.4	22.3	5.5	2.1	0.8
14	20.4	0.5	22.5	5.9	2.1	1.0
18	20.6	0.7	22.7	6.7	2.1	1.2
22	20.9	0.8	22.9	6.7	2.0	1.5
26	20.9	0.6	21.6	3.5	0.7	1.6
30	21.0	0.4	21.5	2.5	0.5	1.6

compression isotherm at the $T = 30$°C. This is due to the change of the monolayer phase from the tilted-condensed phase of the AA monolayer at the subphase temperature $T = 10$°C and 22°C to the liquid-expanded phase at $T = 30$°C. Such behavior can be associated with an increase in the contribution from the interaction of the head groups of surfactant molecules with each other to the intermolecular interaction in the monolayer during its compression [34-36] and a decrease in the length of the tilted-condensed phase region of the monolayer on the compression isotherm (ΔA_0) [37,38]. The described effect is associated with the appearance of NiArch clusters under the AA monolayer [39]. Compression of the AA monolayer leads to a change in the distance between Ni clusters and the formation of their aggregates under the surface of the subphase. This, in turn, leads to the appearance of inhomogeneity in the distribution of surface pressure. As a result of the subphase heating, the number of new points of NiArch clusters growth increases, and the type of the liquid phase of the AA monolayer changes.

A change in the temperature of the subphase also affects the untilted-condensed phase of the AA monolayer. Thus, an increase in the temperature of the subphase leads, on the whole, to a change in the properties of the AA monolayer itself. It can be seen that the A_{CN} reaches the maximum value at 30°C and

k_C reaches the minimal value at 22°C (Table 1). For the untilted-condensed and tilted-condensed phases, the values of k_C and k_L take maximal values at temperatures of 10°C and 30°C (Table 1). This can be explained as follows. It is well known that the rate of a chemical reaction has an exponential temperature dependence [40]. In our case, a decrease in the temperature of the subphase leads to a slowdown in the reaction rate of the formation of NiArch. In this regard, the properties of the NiArch monolayer slightly differ from the properties of the AA monolayer. An increase in the subphase temperature leads to an increase in the efficiency of the exchange reaction and an increase in the homogeneity of the monolayer due to the appearance of new centers of growth of NiArch clusters [34,41].

3.3. Morphology of LB films based on AA monolayers with NiArch clusters

The images of the AA LB film and its profile line height are shown in **Fig. 4**. The film has a homogeneous morphology with alterations in profile height close to 2 nm that is comparable with the length of the AA molecule 2.25 nm. The defects in the film are explained by the structural rearrangements in the film during its drying.

The length of the tilted-condensed phase region on the compression isotherm ($\varDelta A_0$) is one of the most important parameters of a monolayer. Its analysis makes it possible to judge the intensity and efficiency of the salt formation reaction in the monolayer. From Table 1 it can be seen that the most dramatic change in $\varDelta A_0$ occurs at a subphase temperature above 26°C. This may be related both to the appearance of new growth centers of NiArch clusters and to a change in their size with an increase in the subphase temperature. The investigation of the surface morphology of LB films based on AA with NiArch clusters formed at different subphase temperatures was performed to this effect study.

The typical images of the surface of the obtained LB films based on AA monolayers with NiArch nanoparticles formed at different subphase temperatures are shown in **Fig. 5***a*. The right part of Fig. 5*a* shows an enlarged image of a group of NiArch clusters. The inset of Fig. 5*a* shows the surface profile of one NiArch cluster. The NiArch cluster is a cylindrical particle with a large aspect ratio between height and width.

An increase in the subphase temperature leads to an increase in the total number of NiArch clusters (Fig. 5*b*). The series of 7 images of the film surface morphology with dimensions of $40 \times 40\mu$m were obtained to construct a histogram of the distribution of the number of particles by size. Series were obtained for the films formed at subphase temperatures of 10°C, 14°C, 18°C, 22°C, 26°C, and 30°C. The histograms were constructed by using mathematical processing each of the obtained images. Such a histogram
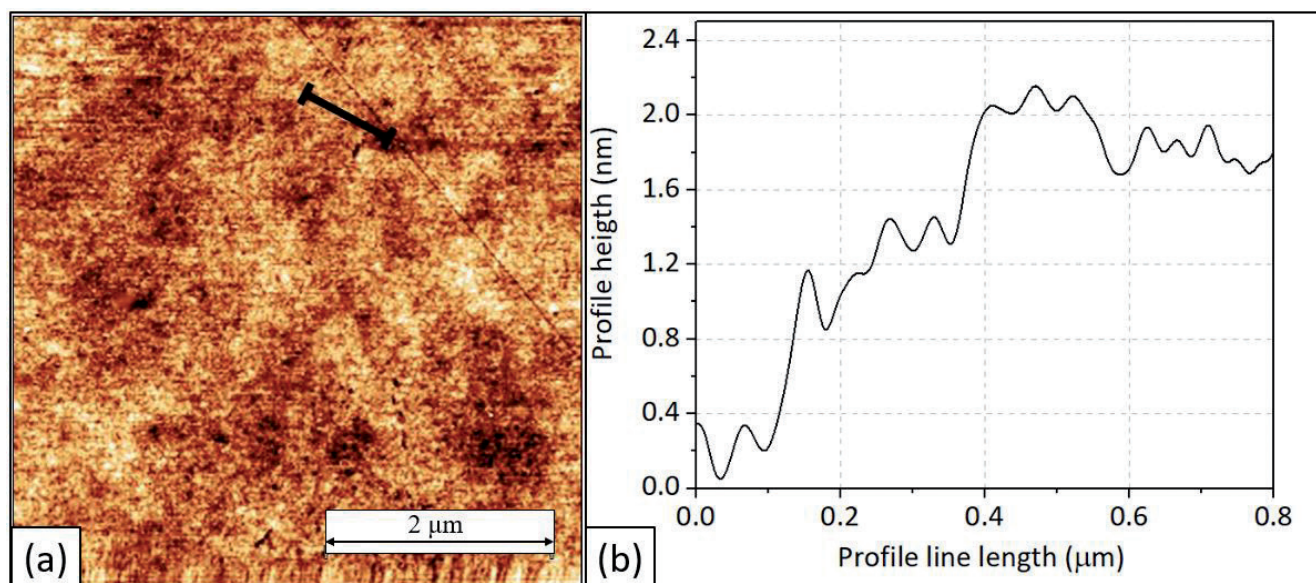

Fig. 4. *An AFM image of AA LB film formed at 22°C on the water subphase in the absence of Ni²⁺ ions (a) and the film profile line (b).*
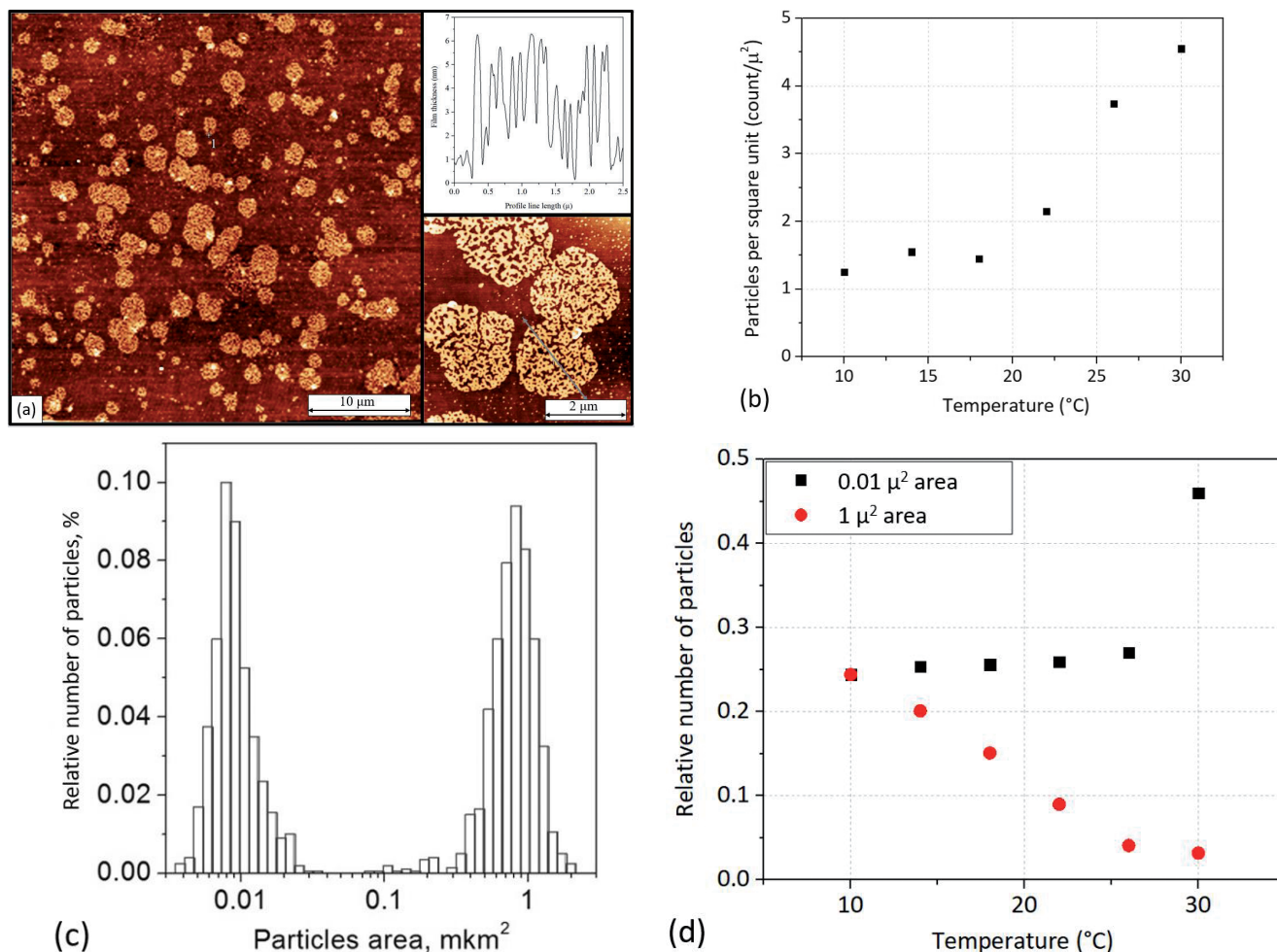
Fig. 5. *(a) An example of AFM image of LB film with NiArch clusters formed at the subphase temperature of 22°C; (b) influence of subphase temperature on numbers of particles per one area init; (c) typical histogram of particles size distribution; (d) Changing of the relative number of NiArch clusters with an occupied area of 0.01 μm².*

for T = 22°C is shown in Fig. 5c. There are two peaks corresponding to NiArch clusters with an area of 1 and 0.01 μm². The number of particles with an area of more than 1 μm² and less than 0.01 μm² was less than 0.05%.

In this regard, NiArch clusters with an area of only 1 μm² and 0.01 μm² were analyzed. The histograms were fitted with a Gaussian distribution (Fig. 5d). It can be seen that at a subphase temperature of 10°C, the number of NiArch clusters with an area of 1 μm² and 0.01 μm² is the same. An increase in the subphase temperature leads to an increase in the number of NiArch clusters with an area of 0.01 μm² and a decrease in the number of NiArch clusters with an area of 1 μm². At a subphase temperature of 30°C, the number of NiArch clusters with an area of 1 μm² becomes minimal.

The temperature dependences of the geometric dimensions and areas occupied by NiArch

clusters in the formed LB films are presented in **Fig. 6.** Despite an increase in the number of the NiArch clusters upon subphase heating (Fig. 5b), the area occupied by NiArch clusters decreases (Fig. 6a). As the subphase temperature increases, the average thickness of the NiArch cluster first increases, reaches a maximum at 22°C, and then decreases (Fig. 6b). The average area of NiArch clusters also decreases monotonically with temperature increasing (Fig. 6c).

The change in the number and average size of NiArch clusters with an increase in the subphase temperature can be explained by the next reasons. As the temperature rises, the efficiency of the exchange reaction between the Ni²⁺ ions in the subphase and the polar part of the AA molecule (carboxyl group) increases. Consequently, the number of new cluster growth centers increases. In this case, the dissolution rate of clusters also
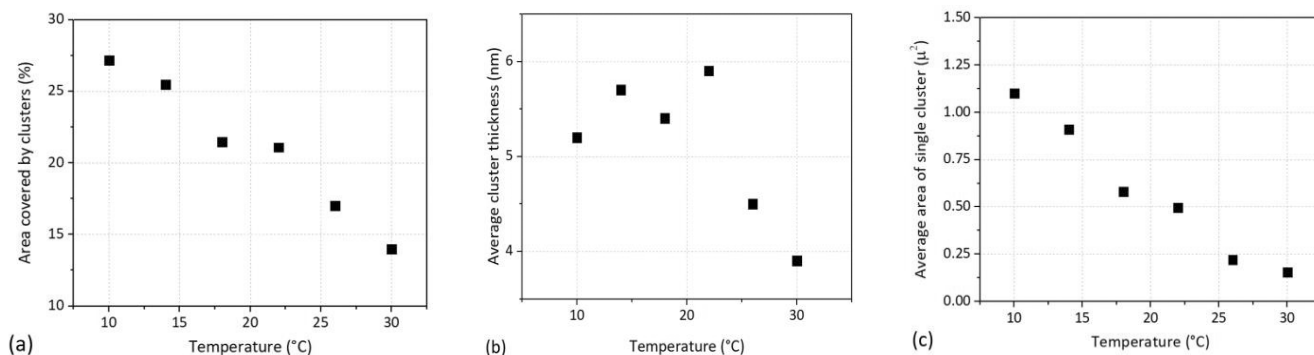
Fig. 6. *The dependencies of (a) film area covered by NiArch clusters, (b) average thickness of NiArch clusters, and (c) average NiArch clusters area (c) on subphase temperature.*

increases at high temperatures, which leads to a decrease in their average area. The subphase heating leads to decreasing cluster sizes (area and thickness). It was found that the horizontal and vertical dissolution rates of the cluster are different. During growth, the cluster is assembled from nuclei of different sizes; therefore, the cluster assembled from them will have a dendrite-like structure with a non-uniform thickness. For this reason, when a cluster is dissolved, the fine fractions located on its periphery first dissolve. This explains the decrease in the area of clusters and the change in the ratio of the number of clusters with areas of $0.01 \ \mu m^2$ and $1 \ \mu m^2$. The dissolution rate of the cluster in thickness is lower, which is explained by the presence of a highly porous dendrite-like structure of the cluster.

These effects can be described by the theory of homogeneous nucleation, which is used to analyze the growth of clusters [36]. This approach implies the existence of a minimum lifetime of clusters during which they dissolve or aggregate to form a stable particle. In this work, the concentration of Ni^{2+} ions in the subphase is far from the saturated concentration. This leads to an insignificant probability of the appearance of nickel derivatives in the volume of the subphase. At the same time, the change in the concentration of Ni^{2+} ions in the interfacial layer occurs as a result of the compression of the AA monolayer with NiArch clusters by movable barriers. This process leads to the formation of NiArch aggregates at the layer boundary. The described effect allows us to consider the system "Langmuir monolayer – the surface layer of the interface" as a supersaturated solution (**Fig. 7**) [40].

In the near-surface layer, due to the adsorption of Ni^{2+} ions by an AA monolayer and its further compression, conditions for an increase in the local concentration of nickel are created. Due to this effect, surface NiArch aggregates are formed at the water-air interface. These aggregates are the seeds for the further growth of clusters. The reaction of the formation of NiArch clusters proceeds continuously from the moment the solution of AA is placed on the surface of the aqueous subphase. At that, an increase in the temperature of the subphase leads to an increase in the rate of the above reaction. In this regard, there is an increase in the number of points of growth of NiArch clusters.
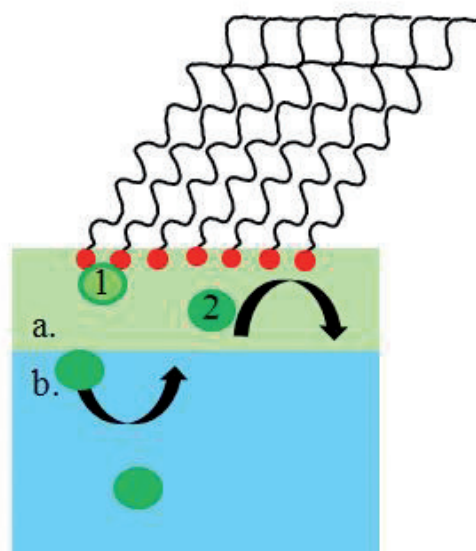

Fig. 7. *Schematic illustration of volume and interfacial layer of water subphase. "a." is an interfacial layer, "b." is a volume of subphase, 1 are Ni^{2+} ions that were reacted with AA molecule and formed a NiArch cluster, 2 are Ni^{2+} ions that were not reacted with acid molecules and could diffuse from interfacial layer to the subphase.*

A decrease in the temperature of the subphase leads to a decrease in the limiting solubility of the nickel chloride salt and a decrease in the dissolution rate of nickel arachidate in the subphase. In this case, the compression of barriers leads to an increase in the average area of NiArch clusters due to their aggregation. The simultaneous influence of these factors leads to the achievement of the critical size of NiArch nuclei when the dissolution process stops.

4. CONCLUSION

The process of formation of clusters of nickel salts under a Langmuir monolayer of arachidic acid (AA) at different temperatures was studied, and the morphology of the corresponding LB films transferred onto a solid substrate was analyzed. It was shown that the change in the number of growth centers of nickel arachidate (NiArch) clusters under the Langmuir AA monolayer can be controlled by the subphase temperature change. It was found that an increase in the subphase temperature in the range from 10°C to 30°C leads to a change in the type of the liquid phase of the AA monolayer with included NiArch clusters and to a decrease in the length of the liquid phase region of the AA monolayer on the compression isotherm. An AA monolayer with incorporated NiArch clusters is in a tilted-condensed phase at a subphase temperature of 10°C. An increase in the temperature of the subphase to 30°C leads to a change in the monolayer phase condition from the tilted-condensed phase to the liquid-expanded phase. This effect can be associated with an increase in the number of growth points of NiArch clusters under the AA monolayer with an increase in the subphase temperature to 30°C.

It was found that an increase in the subphase temperature leads to an increase in the number of NiArch clusters in the LB AA film and a decrease in their size. An increase in the number of NiArch clusters can be associated with an increase in the number of points of their growth with an increase in the temperature of the subphase. Reducing the cluster size, i.e. its average area and thickness is associated with an increase in the dissolution rate of NiArch nuclei in the subphase during its heating. The process of changing the size of a cluster can be described in terms of the theory of nucleation in colloidal solutions. This theory can be applied to our case, taking into account that the nucleation process was localized directly under the monolayer. The factor initiating the process of cluster formation is the change in the intermolecular distance upon compression of the monolayer by barriers. This leads to a change in the local concentration of NiArch molecules in the surface layer and the appearance of NiArch clusters with different sizes. Some of these clusters do not dissolve completely, because their size is large enough and they can to absorb smaller clusters. In general, this leads to an increase in the number and average size of NiArch clusters. However, an increase in the subphase temperature accelerates the dissolution of both large and small clusters. The distribution of NiArch clusters in the formed film was random. However, using the magnetic properties of nickel, they can be structured using external magnetic fields. Using the magnetic properties of NiArch clusters will make it possible to purposefully control the distribution of NiArch clusters in a Langmuir monolayer by an external magnetic field during its formation.

The results obtained are of great importance for the creation of multilayer composite coatings with controlled properties. These coatings can be further used as sensitive coatings for acoustic and electronic sensors.

REFERENCES

1. Kondalkara VV, Yang SS, Patil PS, Choudhury S, Bhosale PN, Lee KK. Langmuir-Blodgett assembly of nanometric WO$_3$ thin film for electrochromic performance: A new way. *Materials Letters,* 2017, 194:102-106.

2. Li T, Lilja K, Morris RJ, Brandani GB. Langmuir-Blodgett technique for anisotropic colloids: Young investigator perspective. *Journal of Colloid and Interface Science*, 2019, 540:420-438. DOI:10.1016/j.jcis.2019.01.044.

3. Xu L, Tetreault AR, Khaligh HH, Goldthorpe IA, Wettig SD, Pope MA. Continuous Langmuir–Blodgett Deposition and. Transfer by Controlled Edge-to-Edge Assembly of Floating 2D Materials. *Langmuir,* 2019, 35:51-59.

4. Avramov ID, Ivanov GR. Layer by Layer Optimization of Langmuir–Blodgett Films for Surface Acoustic Wave (SAW) Based Sensors for

Volatile Organic Compounds (VOC) Detection. *Coatings,* 2022, 15:669.

5. Silva EA, Braunger ML, Gregori A, Olivati CA. Volatile organic compounds detection by electrical sensors using polyalkylthiophene-based Langmuir–Blodgett films. *Applied Sciences,* 2019, 1(3):1-9. DOI: 10.1007/s42452-019-0187-z.

6. Sołoducho J, Cabaj J, Swist A. Structure and Sensor Properties of Thin Ordered Solid Films. *Sensors,* 2009, 9:7733-7752.

7. L. Caseli. Enzymes immobilized in Langmuir-Blodgett films: Why determining the surface properties in Langmuir monolayer is important? *An Acad Bras Cienc.,* 2018, 9:631-644.

8. Gorbachev IA, Smirnov AV, Glukhovskoy EG, Kolesov VV, Ivanov GR, Kuznetsova IE. Morphology of Mixed Langmuir and Langmuir–Schaefer Monolayers with Covered CdSe/CdS/ZnS Quantum Dots and Arachidic Acid. *Langmuir,* 2021, 37:14105-14113. DOI: 10.1021/acs.langmuir.1c02345.

9. Thampi A, Babu K, Verma S. Large scale solvothermal synthesis and a strategy to obtain stable Langmuir–Blodgett film of CoFe2O4 nanoparticles. *Journal of Alloys and Compounds,* 2013, 564:143-150.

10. Villanueva ME, Lanterna AE, Vico RV. Hydrophobic silver nanoparticles interacting with phospholipids and stratum corneum mimic membranes in Langmuir monolayers. *Journal of Colloid and Interface Science,* 2019, 543:247-255. DOI: 10.1016/j.jcis.2019.02.069.

11. Justo Y, Moreels I, Lambert K, Hens Z. Langmuir–Blodgett monolayers of colloidal lead chalcogenide quantum dots: morphology and photoluminescence. *Nanotechnology,* 2010, 21:295606-295612.

12. Hupfer ML, Kaufmann M, Roussille L, Preish J, Weish D, Hinrichs K, Deckert V, Dietzek B, Beckert R, Presselt M. Arylic versus Alkylic-Hydrophobic Linkers Determine the Supramolecular Structure and Optoelectronic Properties of Tripodal Amphiphilic Push-Pull Thiazoles. *Langmuir,* 2019, 35:2561-2570.

13. Al-Ali F, Dejugnat C, Etemad-Moghadam G, Rico-Lattes I. Langmuir films of (alpha-amino) phosphorus amphiphiles on various ion-containing subphases. *Journal of Colloid and Interface Science,* 2004, 273(2):512–516.

14. Protasov DY, Jian WB, Svit KA, Duda TA, Teys SA, Kozhuhov AS, Sveshnikova LL, Zhuravlev KS. Formation of Arrays of Free-Standing CdS Quantum Dots Using the Langmuir–Blodgett Technique. *J. Phys. Chem. C,* 2011, 115:20148-20152.

15. Yanklovich MA, Ivanov NS, Sukhodolov NG, Zhukov AN. A study of the properties and composition of stearic acid monolayers on an aqueous subphase containing cadmium ions. *Colloid Journal,* 2016, 78(2):277-280.

16. Capistran BA, Blanchard GJ. Effects of Cu(II) on the Formation and Orientation of an Arachidic Acid Langmuir-Blodgett Film. *Langmuir,* 2019, 35:3346-3353. DOI: 10.1021/acs.langmuir.9b00022.

17. Vaknin D, Bu W, Satija SK, Travesset A. Ordering by Collapse: Formation of Bilayer and Trilayer Crystals by Folding Langmuir Monolayers. *Langmuir,* 2007, 23:1888-1897.

18. Khomutov GB, Bykov IV, Gainutdinov RV, Polyakov SN, Sergeyev-Cherenkov AN, Tolstikhina AL. Synthesis of Ni-containing nanoparticles in Langmuiur-Blodgett films. *Colloids and Surfaces A: Physicochemical and Engineering Aspects,* 2002, 198:559-567. DOI: 10.1016/S0927-7757(01)00961-X.

19. Chumakov A, Al-Alwani1 AJ, Ermakov A, Shinkarenko J, Begletsova N, Glukhovskoy E, Santer S. The Formation of arachidic acid Langmuir monolayers on the NiCl2 solution. *Journal of Physics: Conference Series,* 2018, 1124:081009.

20. Al-Alwani AJ, Mironyuk VN, Pozharov MV, Gavrikov MV, Glukhovskoy EG. Formation and phase behavior of porphyrin/arachidic acid mixed systems and morphology study of Langmuir-Schaefer thin films. *Soft Materials,* 2022, 20:310-321. DOI:10.1080/1539445X.2022.2028829.

21. Sah BK, Kundu S. Ccollapse of langmuir monolayer formed by the mixture of short- and long-tailed fatty acid molecules. *Colloid and Interface Science Communications,* 2020, 36:100261.

22. Klimova SA, Sreij R, Bratashov D, Bookhold J, Teichert N, Gorobets AS, Hellweg T. Pb arachidate Langmuir-Blodgett coatings of silicon wafers: relation between Pb particle density and

subphase composition *Colloid and Polymer Science,* 2018, 296:771-780.

23. Krajewska M, Dopierała K, Prochaska K. Lipid-protein interactions in langmuir monolayers under dynamically varied conditions. *J. Phys. Chem. B.,* 2020, 124:302-311; doi: 10.1021/acs.jpcb.9b10351.

24. Klimova SA, Stetsyura SV, Venig SB, Kaya M, Dincer I, Elerman Y, Skaptsov AA. The effect of Langmuir arachidic acid layers on surface morphology and electrical properties of a polycrystalline CdS film. *Int. J. Nanotechnol.,* 2018, 15:402-416. DOI: 10.1504/IJNT.2018.094797.

25. Khomutov GB. Two-dimensional synthesis of anisotropic nanopartocles. *Colloids and Surfaces A: Physicochemical and Engineering Aspects,* 2002, 202:243-267.

26. Zarenezhad E, Abdulabbas HT, Marzi M, Ghazy E, Ekrahi M, Pezeshki B, Ghasemian A, Moawad AA. Nickel Nanoparticles: Applications and Antimicrobial Role against Methicillin-Resistant Staphylococcus aureus Infections. *Antibiotics,* 2022, 11(9):1208.

27. Betts JJ, Pethica BA. The ionization characteristics of monolayers of weak acids and bases. *Trans. Farad.Soc.,* 1956, 52:1581-1589.

28. Vollhardt D, Fainerman VB. Progress in characterization of Langmuir monolayers by consideration of compressibility. *Advances in Colloid and Interface Science,* 2006, 127:83-97.

29. Podolskaya EP, Serebryakova MV, Krasnov KA, Grachev SA, Gzgzyane AM, Sukhodolov NG. Application of Langmuir–Blodgett technology for the analysis of saturated fatty acids using the MALDI-TOF mass spectrometry. *Mendeleev Commun.,* 2018, 28:337-339.

30. Khomutov GB, Gainutdinov RV, Gubin SP, Kislov VV, Khanin VV, Rakhnyanskaya AA, Sergeev-Cherenkov AN, Soldatov ES, Suyatin DB, Taranov IV, Tolstikhina AL. Organized planar nanostructures from ligand-stabilized nanoclusters: a route to molecular nanoelectronic devices. *Applied Surface Science,* 2004, 566-568, 396–401.

31. Khomutov GB, Gubin SP. Interfacial synthesis of noble metal nanoparticles. *Materials Science and Engineering C,* 2002, 22(2):141-146. DOI: 10.1016/S0928-4931(02)00162-5.

32. Ellis JW, Pauley JL. The infrared determination of the composition of stearic acid multilayers deposited from salt substrata of varying pH. *J. Colloid Sci.,* 1964, 19:755.

33. Gorbachev IA, Shtykov SN, Brezesinski G, Glukhovskoy EG. Studying of Quantum Dots Langmuir Monolayers Stability at the Different Subphase Temperature. *BioNanoSci,* 2017, 7:686-691.

34. Johann R, Brezesinski G, Vollhardt D, Möhwald H. The effect of headgroup interactions on structure and morphology of arachidic acid monolayers. *J. Phys. Chem. B,* 2001, 105: 2957-2965.

35. Gaines GL. I*nsoluble Monolayers at Liquid-Gas Interfaces.* New York, Interscience Publ., 1966, 386 p.

36. Adamson AW. *Physical chemistry of surfaces.* New York, Wiley Publ., 1983, 698 p.

37. Koerner RM, Lord AE, Hsuan YH. Arrhenius modeling to predict geosynthetic degradation. *Geotext Geomembr.,* 1992, 11(2):151-183; doi: 10.1016/0266-1144(92)90042-9.

38. Smith IWM. The temperature-dependence of elementary reaction rates: beyond Arrhenius. *Chem. Soc. Rev.,* 2008, 37:812-826.

39. Dhanabalan A, Riul AJr, Mattoso LCH, Oliveira ONJr. Composite Langmuir monolayers and Langmuir-Blodgett films from 16-mer polyaniline. *Langmuir,* 1997, 13:4882-4886.

40. Carvalho-Silva VH, Coutinho ND, Aquilanti V. Temperature Dependence of Rate Processes Beyond Arrhenius and Eyring: Activation and Transitivity. *Front. Chem.,* 2019, 7:1-11.

41. Andelman D, Brochard F, Knobler C, Rondelez F. Structures and Phase Transitions in Langmuir Monolayers. In: Gelbart W.M., Ben-Shaul A., Roux D. (eds) *Micelles, Membranes, Microemulsions, and Monolayers, Partially Ordered Systems.* New York, Springer, 1994.

42. Ter-Minassian-Saraga L. Recent work on spread monolayers, adsorption and desorption. *Journal of Colloid Science,* 1956, 11:398-418.